

Received: 14 February 2022, Accepted: 14 June 2022

Edited by: K. Daniels, L. A. Pugnali, J. Zhao

Reviewed by: J. Douglas - University of Pennsylvania, USA

Licence: Creative Commons Attribution 4.0

DOI: <https://doi.org/10.4279/PIP.140011>

ISSN 1852-4249

Future challenges on focused fluid migration in sedimentary basins: Insight from field data, laboratory experiments and numerical simulations

A Gay^{1*}, V Vidal^{2†}

In a present context of sustainable energy and hazard mitigation, understanding fluid migration in sedimentary basins – large subsea provinces of fine saturated sands and clays – is a crucial challenge. Such migration leads to gas or liquid expulsion at the seafloor, which may be the signature of deep hydrocarbon reservoirs, or precursors to violent subsea fluid releases. If the former may orient future exploitation, the latter represent strong hazards for anthropic activities such as offshore production, CO₂ storage, transoceanic telecom fibers or deep-sea mining. However, at present, the dynamics of fluid migration in sedimentary layers, in particular the upper 500 m, still remains unknown in spite of its strong influence on fluid distribution at the seafloor. Understanding the mechanisms controlling fluid migration and release requires the combination of accurate field data, laboratory experiments and numerical simulations. Each technique shall lead to the understanding of the fluid structures, the mechanisms at stake, and deep insights into fundamental processes ranging from the grain scale to the kilometers-long natural pipes in the sedimentary layers. Here we review the present available techniques, advances and challenges still open for the geosciences, physics, and computer science communities.

I Introduction

Fluids (water, gases, CO₂, sulphides, hydrogen, hydrocarbons) migrating through pipes in sedimentary basins and being expelled at the seafloor is a widespread process which is gaining increased attention in the assessment of geohazards, for environment conservation [1], and for securing fossil energy resources. Pipes (or chimneys) are very common in sedimentary basins and they are interpreted as focused fluid flow structures which hydraulically connect deep sources with the sedimentary cover

leading to the formation of various seafloor fluid seep structures such as pockmarks, mud-volcanoes and injectites [2–4]. Pockmarks are generally developing in unconsolidated fine-grained sediments as cone-shaped circular or elliptical depressions (negative relief compared to the regional slope), due to fluid migration and expulsion (Fig. 1). Mud volcanoes and sand extrudites-injectites are due to a mix of fluid and mud or sand migrating from buried overpressured (pressure that exceeds the normal hydraulic pressure at depth) mud-rich or sand-rich reservoirs, respectively, forming a dome structure at the seafloor (a positive relief compared to the regional slope) (Fig. 1). They range from a few metres to 2 km or more in diameter and from a few m to hundreds of m in height [5]. Because of the nature and relatively low temperature of the fluids expelled, they are called cold seeps, supporting methane- and sulphide-dependant biological com-

* aurelien.gay@gm.univ-montp2.fr

† valerie.vidal@ens-lyon.fr

¹ Géosciences Montpellier, Université de Montpellier, CNRS, Université des Antilles, Montpellier, France.² ENSL, CNRS, Laboratoire de Physique, F-69342 Lyon, France.

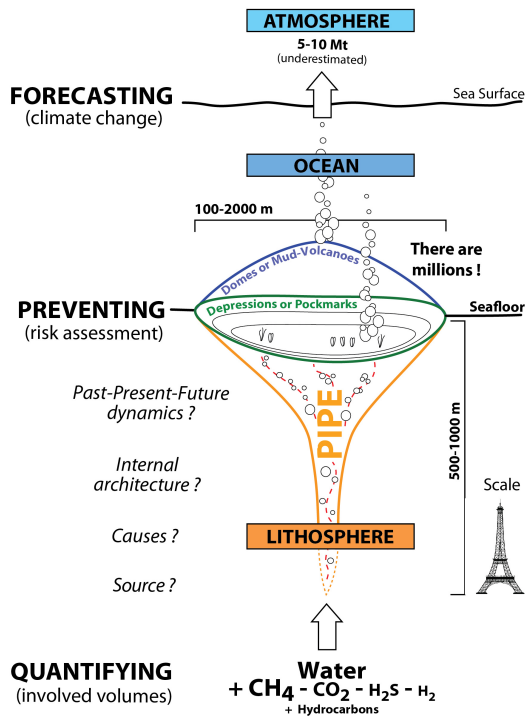


Figure 1: Sketch representing the challenges on fluid migration through pipes in sedimentary basins. From a physicist’s point of view, the host medium (lithosphere) can be viewed as liquid-saturated grains.

munities (see [6] and references therein).

For the last decade, increasing exploration/production and consumption of fossil fuels has led to tremendous greenhouse gas emissions (CO_2 , methane, etc.), causing a rise in the global temperature level [7] and severe natural hazards [8]. Methane (CH_4) is a powerful greenhouse gas whose natural and anthropogenic emissions contribute $\sim 20\%$ to global radiative forcing (Pachauri *et al.*, 2015) [9]. Current annual global methane emissions sourced from natural geological sources are estimated at 18–63 Mt, with offshore seeps contributing 5–10 Mt, there being considerable uncertainty in these estimates [10,11].

In spite of its importance, the subject still suffers from a lack of interdisciplinary studies incorporating geologists, oceanographers, physicists and geophysicists, chemists and geochemists, biologists, mineralogists, and sandbox/numerical modellers.

Combination of these research topics in constraining the physical properties of fluid pathways and the mechanisms of fluid flow is an outstanding opportunity to 1) study the dynamical processes involved in the formation of fluid pipes and focused fluid flow systems, 2) evaluate the dynamics of resources (including gas hydrates), 3) prevent submarine slope failures and related tsunamis through risk assessment, 4) constrain driving mechanisms and quantification of expelled fluid volumes through pipes, 5) understand the occurrence of chemosynthetic benthic ecosystems that develop in deep seep sites, and 6) better understand coupling between the deep geosphere and the biosphere by quantifying the input of greenhouse gases (e.g. methane & CO_2) into the ocean/atmosphere system, which may influence the atmospheric carbon budget and Earth’s paleo- and present climate (Fig. 1).

For the physicist, fluid migration through pipes in sedimentary basins (Fig. 1) can be seen as a large-scale example of a multiphase flow in a deformable dense granular medium - namely, a frictional multiphase flow. For a non-wetting fluid invading a granular medium immersed in a wetting fluid, the morphology of fluid invasion is determined by the interplay between capillary forces, viscous forces, buoyancy and particle friction and cohesion [12]. The capillary number compares the relative effects of viscous drag forces and surface tension forces, $\text{Ca} = \eta V / \gamma$ where η is the viscosity of the wetting fluid, V the typical invasion velocity and γ the surface tension. The Bond number corresponds to the ratio between gravitational and capillary forces, $\text{Bo} = \Delta \rho g L^2 / \gamma$, with $\Delta \rho$ the density difference between the two fluids (usually, between the surrounding liquid and the invading gas), g the gravitational acceleration and L a characteristic length, usually taken as the pore size. The capillary number is mostly used to classify *horizontal* frictional flows [13], while the Bond number is more classically used to describe the morphology of rising gas in saturated sands [14,15]. However, in spite of their successful application to different invasion geometries, their use becomes limited when dealing with highly polydisperse or cohesive/frictional systems. Other dimensionless numbers have been proposed involving the hydraulic conductivity [16] or the width of the distribution of the capillary overpressure in the system [17,18]. The fracturing num-

ber, initially proposed by Holtzmann *et al.* [19,20], predicts the emergence of a fracturing pattern and was later adapted to buoyancy-driven experiments [21].

When the invading fluid is similar to the fluid initially surrounding the grains, however, most of the above dimensionless numbers are ruled out as capillary forces no longer play a role. In the context of hydraulic fracturing, the threshold is reached when the pore pressure, increasing faster upon the injected flow than its dissipation through the medium, overcomes the tensile strength of the poroelastic medium [22,23]. In most configurations, a continuous fluid injection is uniformly imposed at the base of the granular medium. Although stable, uniform fluidization has been reported before the onset of instabilities [24], it leads in most cases to a focused fluid flow during fluidization, either in monolayer [25, 26] or in multi-layer systems [27]. Recent works in microfluidics have provided additional insights into the importance of bed compaction and dilation, which play a fundamental role in the hysteretic behavior of the sediment bed near fluidization [28]. Localized fluidization has also been investigated for practical applications such as tapered beds [29], leaking pipes [30] or magmatic intrusions [31]. In this configuration, the fluid is injected through a single nozzle at the base of the granular medium leading, in the fluidization regime, to a stable fluidized cavity or a chimney crossing the whole layer [32–35]. To our knowledge, however, there has been no quantitative analysis of the morphology of the fluidized zone over long time lapses. However, localized fluidization is the most probable configuration for pipe formation at depth, resulting from localized fluid escape from a deeper layer.

In this work, we focus on the localized fluidization of a particle medium initially at rest. This scenario corresponds to the formation and evolution of the pipe presented in Fig. 1. In the next sections, we present the most recent state-of-the-art imaging of active fluid pipes (section II.i) as well as information retrieved from analogous fossil fluid pipes in the field (section II.ii). We then introduce two methods to tackle the challenge of fluid focusing on liquid-saturated sands: laboratory experiments (section III.i) and numerical simulations (section III.ii). We focus here on the morphology of the fluidized zone in two-phase systems, show

preliminary results and discuss the challenges. The last section summarizes the most recent advances and perspectives for the future.

II Insights from field data

i Geophysical imagery of active fluid pipes

As the inner crust below the seafloor or ground cannot easily be imaged, geologists and geophysicists have used an indirect method, namely seismic acquisition. The principle is to generate acoustic waves from one of various sources (airguns, explosion, vibrator trucks), propagating in any direction, including below ground. Using receivers to measure time arrivals of waves reflected on buried layers, they are able to reconstruct a vertical seismic section that consists of numerous reflections with location given along the x -axis (horizontal) and two-way traveltimes along the y -axis (vertical). Such an approach has been in long use in the oil industry and is now commonly used in both onshore and off-

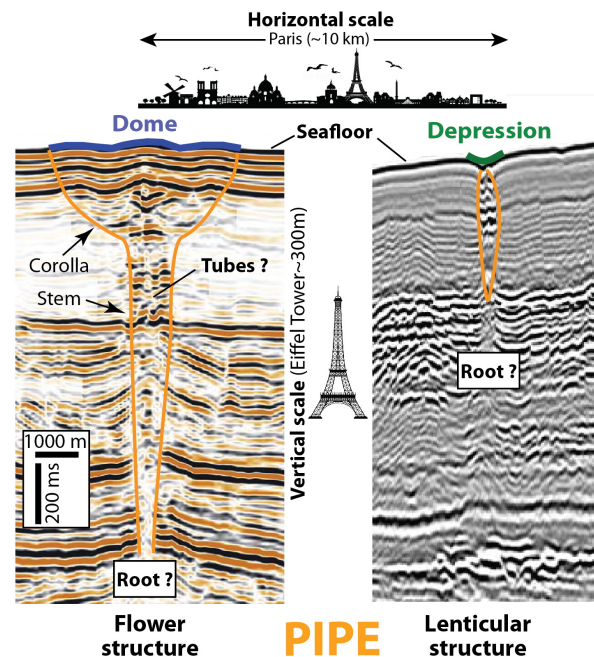


Figure 2: Seismic profiles displaying various fluid pipe structures. Left image from Dumke *et al.*, 2014 [36]; Gay *et al.*, 2012 [37]. Right image from Gay *et al.*, 2006 [38].

shore exploration. Pipes (or chimneys) are usually imaged on seismic sections as systematic disruptions and/or offset of the reflections within vertical zones (Fig. 2), 50–1000 m wide and up to 1000 m high [37–40], forming various shapes such as flower or lenticular structures [37, 39–42].

Although various techniques based on derived attributes and neural network were used to enhance pipes [37, 43–47], neither the internal architecture, nor the root of the pipes were clearly characterized. Even if a genetic link has been established between pipes and supposed underlying sources (structural structures, see [48, 49] and references therein, or buried sedimentary bodies [50–52]), the lack of a precise location of roots leads to a great uncertainty on the feeding source, the related driving processes (underlying overpressure, overlying sediment loading, etc.) or their mutual feed-back. It means that even with the best quality seismic data available today, the interpretation is based on a very simplified picture [53, 54].

The pipes identified on seismic sections are due to gas-charged sediments and to a network of numerous hard carbonate tubes modifying the sound velocity, confirming that the resolution of the actual geophysical imagery is too low. As fluid pipes have never been drilled due to high risk, only passive cores can be recovered for sediment sampling, but they are only 10–15 m long. Fluid fluxes at the seafloor have only be measured using local devices on cores, in the water column or on ROV (Remotely Operated Vehicles) [55, 56]. As for seismic imagery, in situ measurements in the shallow sub-surface give a present-day photograph of fluid fluxes, which is not representative of past emissions. Even a large seafloor tent for integrating fluid fluxes could not be set up for a period of time long enough as the involved processes are active over millions of years [57].

ii Analogous fossil fluid pipes in the field

Even if the internal architecture of pipes cannot be properly imaged using modern geophysical approaches, they could be characterized in the fossil record, once the host sediments have transformed into rocks and they were uplifted by past geodynamic events (tectonic faults, mountains rising etc. . .), allowing human inspection today all along the vertical pipe from source to seep. Surprisingly,

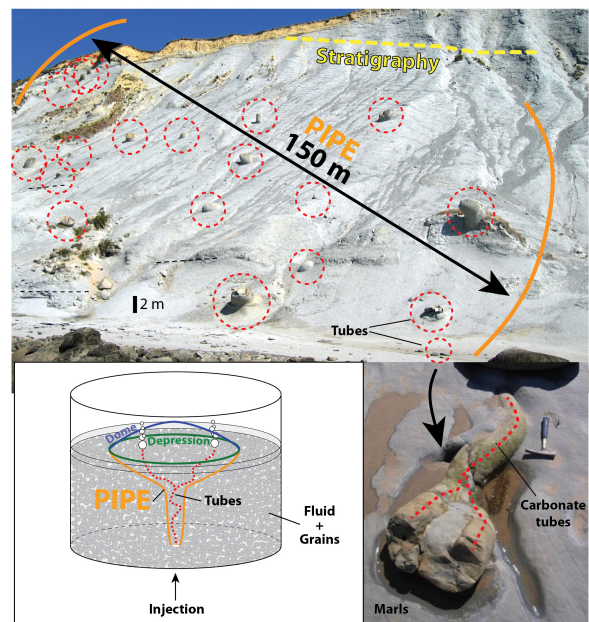


Figure 3: Example of a vast field of tubes, 150 m wide, in Cape Turnagain (New Zealand), which is now interpreted as one single conduit (i.e. a fluid pipe).

given the number and the size of pipes described offshore and given the large number of exhumed fossil paleo-seafloor seep structures reported onshore [58–60], underlying feeding pipes have never been identified in the fossil record. Only a few examples of carbonate tubes have been reported worldwide: in France [57, 61], in Greece [40, 62, 63] and in New-Zealand [64–68]. The tubes are separated from 5 to 30 m, locally connecting to their neighbours and, taken all together, they are organized in a 150–250 m sub-circular area without disrupting the general layering of marls (Fig. 3). A pipe may indeed correspond to the sum of smaller carbonate tubes focusing fluids, coupled to more diffuse migration in a hectometres-wide area.

Reaction-transport modelling (RTM) has shown that authigenic carbonate precipitation is largely controlled by fluid flow intensity and sedimentation rate [69–74] providing the first quantitative insights into the link between carbonate precipitation and upward CH_4 flow [75]. This means that the total volume of expelled fluids can now be deduced directly from the volume of carbonates identified within a seep area. However, such an ap-

proach only gives the total amount of fluids that have migrated through the pipe from its birth to its death. Recent studies conducted in the South-East basin of France have shown that the 800 m wide giant paleo-seep site of Beauvoisin has developed for over 3.4 Ma [57]. They have also shown that periods of active fluid seep alternated with periods of apparent quiescence, about 200 kyr each. Underlying fossil fluid tubes have the same mineralogic and geochemical phases, indicating that they have formed contemporaneously due to the same fluids [61]. Once the carbonate tubes are formed within the underlying feeding pipe, they remain open for a very long period of time (156 Ma), which is of primary importance for the sealing capacity of such “impermeable” intervals in the case of CO₂ or nuclear waste storage. It means that these conduits may contribute to a major leak, carbonate tubes acting as an active plumbing system connecting deep layers (reservoirs) with the ground and the ocean/atmosphere. It is called a seal-bypass system [76]. Field work gives very important information on the 3D reconstruction of the fluid pipes. It also provides clues to the seep activity, but only in a binary mode: 1=seep ; 0=no seep. It does not give any details on the dynamics of the fluids.

III Challenges in the lab

Although the challenges are numerous, insights from field data bring forward the following key questions related to fluid migration in a liquid-saturated granular matrix: What are the physical mechanisms controlling the formation of fluid pipes? How to quantify the origin/volume of fluids at depth based on seafloor observations? To tackle these questions in the laboratory, the method is two-fold: 1) laboratory experiments to reproduce at a smaller scale the complex behavior of multi-phase flows; 2) numerical simulations to control the parameters down to the grain size and quantify the interface phenomena.

i Laboratory experiments

Several authors have used laboratory experiments to study the formation of fluid invasion and piercement structures in different contexts: kimberlite pipes [77], hydrothermal vents [78], mud volcanoes [79], gas seeps [17, 80, 81], magmatic intrusions [82]

or air sparging [15, 83]. Most of these experiments consist of non-cohesive dry or immersed granular material such as glass microbeads or sand in which a fluid (gas or liquid) is locally injected. To mimic the existence of a pressure gradient and the possible importance of buoyancy effects, the fluid is injected at the bottom of the granular layer, and is free to rise and escape at its surface. We do not mention here the huge literature on fluid invasion patterns in other geometries, going back to the pioneering works of Darcy (1856) [84] or Taylor and Saffman (1959) [85]. The initial fluid invasion pattern strongly varies depending on the experimental parameters, ranging from percolation (no displacement of the granular matrix) to fracture [18, 86] or even, for sufficiently high fluid overpressure, a conical structure corresponding to the uplift shear zone at short times [78]. However, interestingly, most experiments exhibit a similar fluidization morphology at long times. For 3-phase systems (gas invasion in liquid-saturated sands), the stationary shape of the fluidized zone is a parabola [15, 16, 87, 88], although it has often been mistaken for a cone-shape invasion [18, 88]. To our knowledge, 2-phase systems mostly focus on the fluidization process at short times, and lack statistics in the stationary state to conclude univocally on the fluidized zone morphology.

Although these experiments appear (almost) as easy to set up as playing with sand, they raise many questions when they aim to model the natural phenomena described in section II. First, scaling down to the laboratory scale – or upscaling back to nature – finds its limitation in the narrow range in which the grain size is limited, typically between a few tens of μm to a few mm, attempting to avoid, on the one side, Brownian motion, and on the other side, unrealistically large pores. Confining pressures are much lower compared to those in the field, but viscous pressures are also lower, making it possible to reproduce similar physics, as in the case of hydraulic fracturing. As stated in section I, however, there is not yet any single, relevant dimensionless number to describe the morphology of the fluidized zone either at the laboratory scale or in the field; despite the much lower confining pressures compared to those in the field, the viscous pressures are also lowered.

Second, the particle material, shape, roughness, wettability and polydispersity are among the many

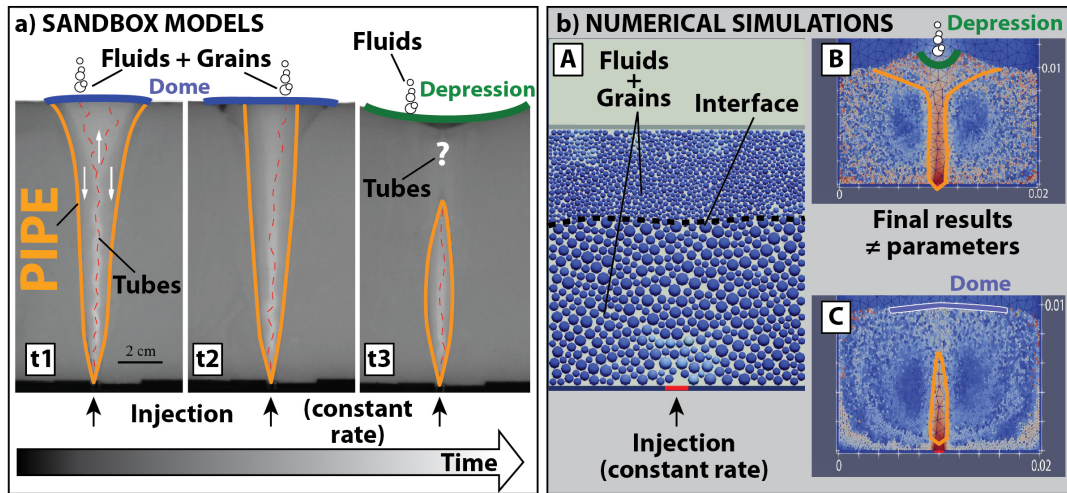


Figure 4: (a) Fluidized zone formed by water injected at constant flow-rate ($Q=50$ mL/min) at the base of a granular layer (glass beads $106\text{--}212\ \mu\text{m}$) immersed in water. t_1 , t_2 , t_3 indicate successive times ($t_3 \simeq 2.5$ h). At short times (t_1), the lower part of the fluidized zone is a vertical narrow zone while the upper part is wider, analogous to the stem and corolla described in section II.i. (b) (A) Modeling an interface between coarse (bottom) and fine (top) grains. (B) Full fluidization or (C) formation of a cavity for an initially homogeneous granular layer immersed under water (5000 particles, radius $200\ \mu\text{m}$, cell dimensions indicated in m, 25 s simulations). The water injection velocity through the central bottom point is (B) $v = 2 \times 10^{-2}$ m/s and (C) $v = 1.5 \times 10^{-2}$ m/s.

parameters which may have a direct influence on fluid migration and the formation of structures. Finally, most granular media are opaque, prohibiting direct visualization of the fluid invasion pattern. This last drawback can be overcome by working in a confined environment (Hele-Shaw cell), ensuring a direct visualization by light transmission but introducing possible wall interaction effects. Technical developments have made it possible to extend direct fluid flow visualization to 3D experiments with refractive index-matching (RIM) with light-transmission [89, 90] or coupled with Planar Laser-Induced Fluorescence (PLIF) [91–94], magnetic resonance imaging (MRI) [95] or X-Ray tomography [82].

In spite of these limitations, analogue experiments make it possible to access spatial and temporal scales which may not be achieved by numerical simulations. In addition, they account inherently (1) for the coupling between the physical processes at stake and (2) for large deformations, complex rheological behavior of dense polydisperse packings [96], transition from laminar to turbulent flows, and many other effects which still challenge theoretical

or numerical predictions.

Here, we present preliminary results of localized fluidization in a granular medium, by injecting water in an initially water-saturated sand. These results do not aim at being exhaustive, but at pointing out puzzling behaviors in an apparently simple system, and challenges still to overcome. Figure 4a presents the experimental observation of the formation of a fluidized zone by injecting water at the bottom of an immersed granular layer. Experiments are performed in a Hele-Shaw cell ($356\ \text{mm} \times 295\ \text{mm}$, gap $3\ \text{mm}$) initially filled with spherical glass beads ($106\text{--}212\ \mu\text{m}$, USF Matrasur) immersed in water. At time $t = 0$, water is injected at constant flow-rate Q through a nozzle (inner diameter $1\ \text{mm}$) at the bottom, by means of a pump coupled to a flow-rate controller (Bronkhorst, mini CORI-FLOW). Direct visualization is performed by a light source (transparency flat viewer, Just NormLicht) located behind the experiment, and a camera (BASLER) in front. This technique makes it possible to evidence the granular layer and inner grain motion by intensity contrast – the darker the image, the more important the grain packing frac-

tion. In the fluidization regime, at short times, the lower part of the fluidized zone is a vertically extended narrow zone while the upper part is wider, analogous to the stem and corolla described in section II.i (Fig. 4a, t_1). Running the experiment over longer time lapses shows the evolution of the fluidized zone morphology. The upper part narrows (Fig. 4a, t_2) until it eventually closes, leading to the formation of a lenticular fluidized cavity stable over the experimental time (Fig. 4a, t_3). This puzzling result, still under investigation, shows the richness and sometimes surprising complexity of fluid migration behavior inside liquid-saturated sands. However, it is experimentally difficult, if not impossible, to control precisely the local grain packing, to quantify the force chains, etc. It is therefore interesting to complement this approach by numerical simulations.

ii Numerical simulations

Several authors have attempted to numerically simulate fluid pipe initiation and propagation into overlying layers. They involved porosity waves as the main mechanism for the formation of pipes [97–105]. Porosity waves occur as a result of fluid flow instability enhanced by strong interaction between the fluid flow and viscous matrix deformation [105–109]. In the absence of chemical reactions and high shear strains, focused fluid flow is generated due to non-symmetrical dilation and compaction of the pore space, where the latter is delayed compared to its dilation [110–112]. Viscoelastic rocks further sustain the upward propagation of such pipes, its direction being defined by pressure gradient and gravity. The viscous compaction time scale, which depends on the difference between solid and fluid densities creating buoyancy forces, controls the upward pipe propagation. These structures are produced by arching or diapiric intrusion into the overlying sediments along high permeability channels, such as zones of mechanical weakness, like fractures and faults [113, 114]. However, such structures are more related to mud diapirs and mud volcanoes as they are piercement structures formed by high subterranean pressure imposed on ductile material in deep basins hosting relatively thick sedimentary sequences [115]. As shown in fossil analogues, they do not represent fluid pipes.

Contrary to laboratory experiments, numerical

simulations provide accurate control over grain shape, packing, and the boundary conditions. However, they are limited by 1) the system size – the larger the number of particles, the higher the computational cost; 2) the adequate coupling between the physical mechanisms, in particular the fluid-grains interactions; 3) the dilemma in choosing a high spatial and temporal resolution, which limits the system evolution to short time scales or face unrealistically long computational times.

Recently, we have used the LMGC90, an open platform dedicated to the modelling of large collections of interacting objects in 2D and 3D [116, 117]. It aims at modelling objects of any shape with various mechanical behaviour and to take into account interaction laws as complex as necessary. Furthermore, multi-physics couplings (thermal effects, fluids, etc) can be taken into account. LMGC90 is designed as a research software which offers to developers the possibility to add new physical models (behaviour law, interaction law, etc), numerical models (finite element, natural element, etc), technical features (contact detection, visualization, parallelism, etc) and numerical strategies (time integration, numerical solver, etc). Based on this DEM-CFD software, we aim at modelling the initial pipe formation and evolution when injecting a fluid at the base of a liquid-saturated sand (Fig. 4b, A). The first simulations in 2D reproduce qualitatively the different regimes observed in the experiments, in particular the full layer fluidization (Fig. 4b, B) or the formation of a cavity (Fig. 4b, C) for an initially homogeneous granular layer. The current work focuses on modelling an interface between two layers – a challenge accessible to this method, which has recently been developed to capture the interface between two non-miscible fluids during their migration [118].

IV Conclusion and perspectives

In offshore exploration, the thick water column leads to the use of indirect methods, such as geophysical imagery and sampling tools, to get imagery and data of the seafloor and what lies beneath. The deeper the object to be imaged, the lower is its resolution, and models may help in better understanding processes at depth. However, given the fact that the number of clay particles

(< 2 μm) in a cube of 100 m side of sediments typical of continental slopes is of the same order of magnitude as the number of stars in the known universe ($\sim 3 \times 10^{23}$), it is impossible to simulate all grains in models. These latter are generally simplified representations of natural cases and they are used to test ideas and processes. Since models are representations of scientific understandings, as these understandings change, so the models change as well and are constantly redesigned to give improved predictions.

Since the end of the 19th century, scientists have tried to simulate fluid invasion into granular media for various purposes, including in the last two decades fluid migration and expulsion at the seafloor. For instance, Nermoen *et al.* (2010) [78] derived analytical solutions and concluded that fluidization occurs when the seepage forces integrated over the conical fluidized area balance the weight of the granular material [78, 119]. They also noticed that their model overestimated the critical pressures observed in natural examples. The main reason of this overestimation probably comes from the cohesive behaviour of natural materials which could not be simulated by non-cohesive glass beads. In cohesive materials, hydraulic fractures form when the fluid pressure reaches a critical value $\sigma_3 + T$, where σ_3 is the minimum stress and T is the tensile strength, which can be smaller than fluid pressure required for fluidization. In a sedimentary basin, at shallow depth (< 1000 m), tensile strength of fine sediments (clays) ranges between 0.2 to 1.1 MPa for porosity ranging between 0.7 and 0.4 [120]. These small, but not null, values of cohesion may modify the piercement morphologies of fluid pipes. Fundamental attempts to describe fluidization in cohesive granular media mainly focused on gas invading dry materials [124]. In this configuration, laboratory experiments pointed out different regimes: low-cohesive grains mostly displayed expansion and pipe formation, while cohesive sediments exhibited uplift and tensile fractures [125]. A more detailed experimental and numerical study by Galland *et al.* [126] pointed out the importance of two dimensionless parameters, (1) the ratio between the fluid pressure and the gravitational stress, and (2) the fluid pressure-to-host rock strength ratio. They have shown that low-energy systems result in fracturing and V-shaped vent, while high-energy systems are characterized by cir-

cular pipes resulting from plastic yielding of the host rock. To our knowledge, however, no investigation of piercement structures have been reported for a cohesive material immersed in a fluid. A recent work by Seiphoori *et al.* [127] considered sedimentation for attractive particles, and underlined the critical interplay between the particle interaction and the liquid flow out of the gel-like structure. Clay gels, in particular, exhibit fracture-like channels during the collapse phase of sedimentation. This fascinating behavior opens many questions regarding the role of particle interaction on the morphodynamics of piercement structures in liquid-driven configurations.

In numerical experiments, three types of models are currently developed 1) based on hydraulic fracturing hypothesis where overpressured gas in the source rock induces fractures in the overlying rocks, and a network of hydraulic fractures propagates towards the surface as high-permeability conduits [121], 2) based on porosity waves where pipes propagate spontaneously due to complex nonlinear coupling between fluid buoyancy, asymmetric compaction-decompaction of pores, and viscoplastic deformations of sediment matrix [111, 112], and 3) based on fluidization leading to brecciation and erosion processes within the conduit [122, 123]. However, they all account for a complete or partial loss of stratigraphy within focused fluid flow conduits, which is not the case shown in fossil pipes [61].

Furthermore, given the size of the geophysical anomalies described on seismic profiles, 1000 m high and 250 m wide, and the number of fluid seep structures found both in modern and fossil basins, massive pipes have never been identified in the fossil record. This suggests that either the geophysical anomaly is identified only when the fluid ascent is active, or the migration processes are more diffusive through the sediment matrix and the stratigraphy is not affected. This also could mean that fluid-rock interactions are slow processes, contrary to fluid migration, and once fluids pass through sediments they leave no any macroscopic evidences, such as concretions.

The next challenges in both laboratory experiments and numerical models of fluid migration and related fluid pipe formation will be (1) to explore very-low flow rates to better fit with real processes in the geological record; (2) to investigate pierce-

ment structure formation in cohesive media; (3) to develop numerical simulations solving fluid-grains interactions and cohesion in more realistic granular systems, in particular at the interface between two layers of different grain size. Sediments are far from being the mono- or bi-disperse granular assemblies which are typically investigated by the physicists, and rather exhibit alternating lithologies with various grainsizes, chemical and physical properties. The geological world still provides open challenges that only an interdisciplinary approach shall be strong enough to take on.

Acknowledgements - We acknowledge the CNRS–MIPS grant for providing resources for fluid simulations. Two students, Manon Pochet and Antoine Mullor actively participated in laboratory experiments and simulations through their undergraduate internships. The authors thank Douglas Jerolmack for his review which greatly improved the manuscript.

-
- [1] L Stott, B Davy, J Shao, R Coffin, I Pecher, H Neil, P Rose, J Bialas, *CO₂ release from pockmarks on the Chatham Rise-Bounty Trough at the glacial termination*, *Paleoceanogr. Paleoceanogr.* **34**, 1726 (2019).
- [2] Z Anka, C Berndt, A Gay, *Hydrocarbon leakage through focused fluid flow systems in continental margins*, *Mar. Geol.* **332**, 1 (2012).
- [3] A Gay, S Migeon, *Geological fluid flow in sedimentary basins*, *Bull. Soc. Géol. Fr.* **188**, E3 (2017).
- [4] M Huuse, C A L Jackson, P Van Rensbergen, R J Davies, P B Flemings, R J Dixon, *Subsurface sediment remobilization and fluid flow in sedimentary basins: An overview*, *Basin Res.* **22**, 342 (2010).
- [5] A Gay, M Lopez, C Berndt, M Séranne, *Geological controls on focused fluid flow associated with seafloor seeps in the Lower Congo Basin*, *Mar. Geol.* **244**, 68 (2007).
- [6] H Sahling, C Borowski, *et al.*, *Massive asphalt deposits, oil seepage, and gas venting support abundant chemosynthetic communities at the Campeche Knolls, southern Gulf of Mexico*, *Biogeosciences* **13**, 4491 (2016).
- [7] B Ameyaw, L Yao, A Oppong, J K Agyeman, *Investigating, forecasting and proposing emission mitigation pathways for CO₂ emissions from fossil fuel combustion only: A case study of selected countries*, *Energ. Policy* **130**, 7 (2019).
- [8] *Climate change 2013: The physical science basis. Contribution of Working Group I to the Fifth Assessment Report of the Intergovernmental Panel on Climate Change (IPCC)*, Eds. T F Stocker, D Qin *et al.*, Cambridge University Press, New York (2014).
- [9] *Climate change 2014: Synthesis report. Contribution of Working Groups I, II and III to the Fifth Assessment Report of the Intergovernmental Panel on Climate Change (IPCC)*, Eds. R K Pachauri, L Meyer *et al.*, IPCC, Geneva (2015).
- [10] G Etiope, G Ciotoli, S Schwietzke, M Schoell, *Gridded maps of geological methane emissions and their isotopic signature*, *Earth Syst. Sci. Data* **11**, 1 (2019).
- [11] M Sauniois, P Bousquet, B Poulter, *et al.*, *The global methane budget 2000-2012*, *Earth Syst. Sci. Data* **8**, 697 (2016).
- [12] R Juanes, Y Meng, B K Primkulov, *Multiphase flow and granular mechanics*, *Phys. Rev. Fluids* **5**, 110516 (2020).
- [13] B Sandnes, E G Flekkøy, H A Knudsen, K J Måløy, H See, *Patterns and flow in frictional fluid dynamics*, *Nat. Commun.* **2**, 288 (2011).
- [14] M C Brooks, W R Wise, M D Annable, *Fundamental changes in In Situ Air Sparging flow patterns*, *Ground Water Monit. R* **19**, 105 (1999).
- [15] J S Selker, M Niemet, N G McDuffie, S M Gorelick, J Y Parlange, *The local geometry of gas injection into saturated homogeneous porous media*, *Transp. Porous Med.* **68**, 107 (2007).

- [16] X Z Kong, W Kinzelbach, F Stauffer, *Morphodynamics during air injection into water-saturated movable spherical granulates*, Chem. Eng. Sci. **65**, 4652 (2010).
- [17] G Varas, V Vidal, J C Géminard, *Venting dynamics of an immersed granular layer*, Phys. Rev. E **83**, 011302 (2011).
- [18] G Varas, G Ramos, J C Géminard, V Vidal, *Flow and fracture in water-saturated, unconstrained granular beds*, Front. Phys. **3**, 44 (2015).
- [19] R Holtzmann, R Juanes, *Crossover from fingering to fracturing in deformable disordered media*, Phys. Rev. E **82**, 046305 (2010).
- [20] R Holtzmann, M L Szulczewski, R Juanes, *Capillary fracturing in granular media*, Phys. Rev. Lett. **108**, 264504 (2012).
- [21] R Poryles, G Varas, V Vidal, *Stability of gas channels in a dense suspension in the presence of obstacles*, Phys. Rev. E **95**, 062905 (2017).
- [22] M K Hubbert, D G Willis, *Mechanics of hydraulic fracturing*, Pet. Trans. AIME **210**, 153 (1957).
- [23] E Detournay, *Mechanics of hydraulic fractures*, Annu. Rev. Fluid Mech. **48**, 311 (2016).
- [24] J M Ham, S Thomas, E Guazzelli, G M Homsy, M-C Anselmet, *An experimental study of the stability of liquid-fluidized beds*, Int. J. Multiphas. Flow **16**, 171 (1990).
- [25] P Rigord, A Guarino, V Vidal, J-C Géminard, *Localized instability of a granular layer submitted to an ascending liquid flow*, Granul. Matter **7**, 191 (2005).
- [26] T Mörz, E A Karlik, S Kreiter, A Kopf, *An experimental setup for fluid venting in unconsolidated sediments: New insights to fluid mechanics and structures*, Sediment. Geol. **196**, 251 (2007).
- [27] R J Nichols, R S J Sparks, C J N Wilson, *Experimental studies of the fluidization of layered sediments and the formation of fluid escape structures*, Sedimentology **41**, 233 (1994).
- [28] M Houssais, C Maldarelli, J Morris, *Soil granular dynamics on-a-chip: fluidization inception under scrutiny*, Lab Chip **19**, 1226 (2019).
- [29] Y-F Shi, Y S Yu, L T Fan, *Incipient fluidization condition for a tapered fluidized bed*, Ind. Eng. Chem. Fundam. **23**, 484 (1984).
- [30] X Cui, J Li, A Chan, D Chapman, *Coupled DEM-LBM simulation of internal fluidization induced by a leaking pipe*, Powder Technol. **254**, 299 (2014).
- [31] A Carrara, A Burgisser, G W Bergantz, *The architecture of intrusions in magmatic mush*, Earth Planet. Sci. Lett. **549**, 116539 (2020).
- [32] F Zoueshtiagh, A Merlen, *Effect of a vertically flowing water jet underneath a granular bed*, Phys. Rev. E **75**, 056313 (2007).
- [33] E P Montellà, M Toraldo, B Chareyre, L Sibille, *Localized fluidization in granular materials: Theoretical and numerical study*, Phys. Rev. E **94**, 052905 (2016).
- [34] S E Mena, L-H Luu, P Cuéllar, P Philippe, J S Curtis, *Parameters affecting the localized fluidization in a particle medium*, AIChE J. **63**, 1529 (2017).
- [35] J Ngoma, P Philippe, S Bonelli, F Radjaï, J-Y Delenne, *Two-dimensional numerical simulation of chimney fluidization in a granular medium using a combination of discrete element and lattice Boltzmann methods*, Phys. Rev. E **97**, 052902 (2018).
- [36] I Dumke, C Berndt, G J Crutchley, S Krause, V Liebetrau, A Gay, M Couillard, *Seal bypass at the Giant Gjallar Vent (Norwegian Sea): Indications for a new phase of fluid venting at a 56-Ma-old fluid migration system*, Mar. Geol. **351**, 38 (2014).
- [37] A Gay, R Mourgues, C Berndt, D Bureau, S Planke, D Laurent, S Gautier, C Lauer, D Loggia, *Anatomy of a fluid pipe in the Norway Basin: Initiation, propagation and 3D shape*, Mar. Geol. **332**, 75 (2012).

- [38] A Gay, M Lopez, P Cochonat, M Séranne, D Levaché, G Sermondadaz, *Isolated seafloor pockmarks linked to BSRs, fluid chimneys, polygonal faults and stacked Oligocene-Miocene turbiditic palaeochannels in the Lower Congo Basin*, *Mar. Geol.* **226**, 25 (2006).
- [39] M Hovland, R Heggland, M H De Vries, T I Tjelta, *Unit-pockmarks and their potential significance for predicting fluid flow*, *Mar. Petrol. Geol.* **27**, 1190 (2010).
- [40] H Løseth, L Wensaas, B Arntsen, N M Hanken, C Basire, K Graue, *1000 m long gas blow-out pipes*, *Mar. Petrol. Geol.* **28**, 1047 (2011).
- [41] S M Ruge, N Scarselli, A Bilal, *3D seismic classification of fluid escape pipes in the western Earmouth Plateau, North West Shelf of Australia*, *J. Geol. Soc.* **178**, jgs2020-096 (2021).
- [42] P Van Rensbergen, A Rabaute, A Colpaert, T St Ghislain, M Mathijs, A Brugge-man, *Fluid migration and fluid seepage in the Connemara Field, Porcupine Basin interpreted from industrial 3D seismic and well data combined with high-resolution site survey data*, *Int. J. Earth Sci.* **96**, 185 (2007).
- [43] R Heggland, *Gas seepage as an indicator of deeper prospective reservoirs. A study based on exploration 3D seismic data*, *Mar. Petrol. Geol.* **15**, 1 (1998).
- [44] H Ligtenberg, *Unravelling the petroleum system by enhancing fluid migration paths in seismic data using a neural network based pattern recognition technique*, *Geofluids* **3**, 255 (2003).
- [45] H Ligtenberg, *Detection of fluid migration pathways in seismic data: implications for fault seal analysis*, *Basin Res.* **17**, 141 (2005).
- [46] P Meldahl, R Heggland, B Bril, P De Groot, *The chimney cube, an example of semi-automated detection of seismic objects by directive attributes and neural networks: Part I; Methodology*, *SEG Technical Program Expanded Abstracts*, 931 (1999).
- [47] K M Tingdahl, A H Bril, P F de Groot, *Improving seismic chimney detection using directional attributes*, *J. Petrol. Sci. Eng.* **29**, 205 (2001).
- [48] C Roelofse, T M Alves, J Gafeira, *Structural controls on shallow fluid flow and associated pockmark fields in the East Breaks area, northern Gulf of Mexico*, *Mar. Petrol. Geol.* **112**, 104074 (2020).
- [49] T Velayatham, S P Holford, M A Bunch, R C King, *Fault controlled focused fluid flow in the Ceduna Sub-Basin, offshore South Australia; evidence from 3D seismic reflection data*, *Mar. Petrol. Geol.* **127**, 104813 (2021).
- [50] B Callow, J M Bull, G Provenzano, *et al.*, *Seismic chimney characterisation in the North Sea – Implications for pockmark formation and shallow gas migration*, *Mar. Petrol. Geol.* **133**, 105301 (2021).
- [51] A Gay, M Lopez, P Cochonat, N Sultan, E Cauquil, F Brigaud, *Sinuuous pockmark belt as indicator of a shallow buried turbiditic channel on the lower slope of the Congo basin, West African margin*, *Geol. Soc. London Spec. Publ.* **216**, 173 (2003).
- [52] R Riera, V Paumard, M de Gail, M M Saqab, U Lebrec, S C Lang, A Lane, *Origin of seafloor pockmarks overlying submarine landslides: Insights from semi-automated mapping of 3D seismic horizons (North West Shelf, Australia)*, *Mar. Petrol. Geol.* **136**, 105453 (2022).
- [53] A H Robinson, B Callow, C Böttner, *et al.*, *Multiscale characterisation of chimneys/pipes: Fluid escape structures within sedimentary basins*, *Int. J. Greenh. Gas Con.* **106**, 103245 (2021).
- [54] B Schramm, C Berndt, A Dannowski, C Böttner, J Karstens, J Elger, *Seismic imaging of an active fluid conduit below Scanner Pockmark, Central North Sea*, *Mar. Petrol. Geol.* **133**, 105302 (2021).
- [55] H Ondreas, J-L Charlou, K Olu, Y Fouquet, P Cochonat, A Gay, B Dennielou, J-P Donval, A Fifis, T Nadalig, M Sibuet, *ROV study*

- of a giant pockmark on the Gabon continental margin, *Geo-Mar. Lett.* **25**, 281 (2005).
- [56] M Longo, G Lazzaro, C G Caruso, V Radulescu, R Radulescu, S S Sciré Scappuzzo, D Birot, F Italiano, *Black Sea methane flares from the Seafloor: Tracking outgassing by using passive acoustics*, *Front. Earth Sci.* **9**, 678834 (2021).
- [57] A Gay, M Lopez, J L Potdevin, V Vidal, G Varas, A Favier, N Tribovillard, *3D morphology and timing of the giant fossil pockmark of Beauvoisin, SE Basin of France*, *J. Geol. Soc.* **176**, 61 (2019).
- [58] K A Campbell, *Hydrocarbon seep and hydrothermal vent paleoenvironments and paleontology: Past developments and future research directions*, *Palaeogeogr. Palaeocl.* **232**, 362 (2006).
- [59] S Kiel, *The fossil record of vent and seep mollusks*, In: *The Vent and Seep Biota: Aspects from Microbes to Ecosystems*, Ed. S Kiel, Springer, Heidelberg (2010).
- [60] B M A Teichert, B van de Schootbrugge, *Tracing Phanerozoic hydrocarbon seepage from local basins to the global Earth system*, *Palaeogeogr. Palaeocl.* **390**, 1 (2013).
- [61] A Gay, A Favier, J L Potdevin, *et al.*, *Poly-phased fluid flow in the giant fossil pockmark of Beauvoisin, SE basin of France*, *BSGF - Earth Sci. Bull.* **191**, 35 (2020).
- [62] N M Hanken, R G Bromley, J Miller, *Plio-Pleistocene sediments in coastal grabens, north-east Rhodes, Greece*, *Geol. J.* **31**, 271 (1996).
- [63] R Løvlie, N M Hanken, *Conglomerate test of non-lithified Plio-Pleistocene marine sediments suggests pDRM type remagnetisation*, *Phys. Chem. Earth* **27**, 1121 (2002).
- [64] B Ledésert, C Buret, F Chanier, J Ferrière, P Recourt, *Tubular structures of northern Wairarapa (New Zealand) as possible examples of ancient fluid expulsion in an accretionary prism: Evidence from field and petrographical observations*, *Geol. Soc. London Spec. Publ.* **216**, 95 (2003).
- [65] K Faure, J Greinert, J S von Deimling, D F McGinnis, R Kipfer, P Linke, *Methane seepage along the Hikurangi Margin of New Zealand: Geochemical and physical data from the water column, sea surface and atmosphere*, *Mar. Geol.* **272**, 170 (2010).
- [66] S L Nyman, C S Nelson, *The place of tubular concretions in hydrocarbon cold seep systems: Late Miocene Urenui Formation, Taranaki Basin, New Zealand*, *AAPG Bull.* **95**, 1495 (2011).
- [67] P Malié, J Bailleul, F Chanier, R Toullec, G Mahieux, V Caron, B Field, R Ferreira Mählmann, S Potel, *Spatial distribution and tectonic framework of fossil tubular concretions as onshore analogues of cold seep plumbing systems, North Island of New Zealand*, *BSGF* **188**, 25 (2017).
- [68] S J Watson, J J Mountjoy, P M Barnes, *et al.*, *Focused fluid seepage related to variations in accretionary wedge structure, Hikurangi margin*, *Geology* **48**, 56 (2020).
- [69] R Luff, K Wallmann, *Fluid flow, methane fluxes, carbonate precipitation and biogeochemical turnover in gas hydrate-bearing sediments at Hydrate Ridge, Cascadia Margin: Numerical modeling and mass balances*, *Geochim. Cosmochim. Ac.* **67**, 3403 (2003).
- [70] G Aloisi, K Wallmann, S M Bollwerk, A Derkachev, G Bohrmann, E Suess, *The effect of dissolved barium on biogeochemical processes at cold seeps*, *Geochim. Cosmochim. Ac.* **68**, 1735 (2004).
- [71] R Luff, K Wallmann, G Aloisi, *Numerical modeling of carbonate crust formation at cold vent sites: Significance for fluid and methane budgets and chemosynthetic biological communities*, *Earth Planet. Sci. Lett.* **221**, 337 (2004).
- [72] R Luff, J Greinert, K Wallmann, I Klauke, E Suess, *Simulation of long-term feedbacks from authigenic carbonate crust formation at cold vent sites*, *Chem. Geol.* **216**, 157 (2005).
- [73] D Karaca, C Hensen, K Wallmann, *Controls on authigenic carbonate precipitation at*

- cold seeps along the convergent margin off Costa Rica*, *Geochem. Geophys. Geosyst.* **11**, Q08S27 (2010).
- [74] D Karaca, T Schleicher, C Hensen, P Linke, K Wallmann, *Quantification of methane emission from bacterial mat sites at Quepos Slide offshore Costa Rica*, *Int. J. Earth Sci.* **103**, 1817 (2014).
- [75] J-P Blouet, S Arndt, P Imbert, P Rognier, *Are seep carbonates quantitative proxies of CH₄ leakage? Modeling the influence of sulfate reduction and anaerobic oxidation of methane on pH and carbonate precipitation*, *Chem. Geol.* **577**, 120254 (2021).
- [76] J Cartwright, M Huse, A C Aplin, *Seal bypass system*, *AAPG Bull.* **91**, 1141 (2007).
- [77] A L Walters, J Phillips, R J Brown, M Field, T Gernon, G Stripp, R S J Sparks, *The role of fluidisation in the formation of volcanoclastic kimberlite: Grain size observations and experimental investigation*, *J. Volcanol. Geoth. Res.* **155**, 119 (2006).
- [78] A Neramoen, O Galland, E Jettestuen, K Frisstad, Y Podladchikov, H Svensen, A Malthe-Sørenssen, *Experimental and analytic modeling of piercement structures*, *J. Geophys. Res. Sol. Earth* **115**, (2010).
- [79] A Mazzini, A Neramoen, M Krotkiewski, Y Podladchikov, S Planke, H Svensen, *Strike-slip faulting as a trigger mechanism for overpressure release through piercement structures. Implications for the Lusi mud volcano, Indonesia*, *Mar. Petrol. Geol.* **26**, 1751 (2009).
- [80] G Varas, V Vidal, J C Géminard, *Dynamics of crater formations in immersed granular materials*, *Phys. Rev. E* **79**, 021301 (2009).
- [81] F May, M Warsitzka, N Kukowski, *Analogue modelling of leakage processes in unconsolidated sediments*, *Int. J. Greenh. Gas Cont.* **90**, 102805 (2019).
- [82] S Poppe, E P Holohan, O Galland, N Buis, G Van Gompel, B Keelson, P Y Tournigand, J Brancart, D Hollis, A Nila, M Kervyn, *An inside perspective on magma intrusion: Quantifying 3D displacement and strain in laboratory experiments by dynamic X-ray computed tomography*, *Front. Earth Sci.* **7**, 62 (2019).
- [83] R Semer, J A Adams, K R Reddy, *An experimental investigation of air flow patterns in saturated soils during air sparging*, *Geotech. Geol. Eng.* **16**, 59 (1998).
- [84] H Darcy, *Les fontaines publiques de la ville de Dijon: Exposition et application des principes a suivre et des formules a employer dans les questions de distribution d'eau*, Librairie des corps impériaux des ponts et chaussées et des mines, Paris (1856).
- [85] G I Taylor, P G Saffman, *A note on the motion of bubbles in a Hele-Shaw cell and porous medium*, *Q. J. Mech. Appl. Math.* **12**, 265 (1959).
- [86] R Mourgues, P R Cobbold, *Sandbox experiments on gravitational spreading and gliding in the presence of fluid overpressures*, *J. Struc. Geol.* **28**, 887 (2006).
- [87] W Ji, A Dahmani, D P Ahlfeld, J Ding Lin, E Hill III, *Laboratory study of air sparging: Air flow visualization*, *Groundwater Monit. Remed.* **13**, 115 (1993).
- [88] K R Reddy, S Kosgi, J Zhou, *A review of in-situ air sparging for the remediation of VOC-contaminated saturated soils and groundwater*, *Hazard. Waste Hazard.* **12**, 97 (1995).
- [89] M Stöhr, A Khalili, *Dynamic regimes of buoyancy-affected two-phase flow in unconsolidated porous media*, *Phys. Rev. E* **73**, 036301 (2006).
- [90] Z Sun, C Santamarina, *Grain-displacive gas migration in fine-grained sediments*, *J. Geophys. Res.* **124**, 2274 (2019).
- [91] M J Dalbe, R Juanes, *Morphodynamics of fluid-fluid displacement in three-dimensional deformable granular media*, *Phys. Rev. Appl.* **9**, 024028 (2018).

- [92] S E Mena, F Brunier-Colin, J S Curtis, P Philippe, *Experimental observation of two regimes of expansion in localized fluidization of a granular medium*, *Phys. Rev. E* **98**, 042902 (2018).
- [93] P Philippe, M Badiane, *Localized fluidization in a granular medium*, *Phys. Rev. E* **87**, 042206 (2013).
- [94] M Sarabian, M Firouznia, B Metzger, S Hormozi, *Fully developed and transient concentration profiles of particulate suspensions sheared in a cylindrical Couette cell*, *J. Fluid Mech.* **862**, 659 (2019).
- [95] M H Köhl, G Lu, J R Third, M Häberlin, L Kasper, K P Prüssmann, C R Müller, *Magnetic resonance imaging (MRI) study of jet formation in packed beds*, *Chem. Eng. Sci.* **97**, 406 (2013).
- [96] É Guazzelli, O Pouliquen, *Rheology of dense particle suspensions*, *J. Fluid Mech.* **852**, P1 (2018).
- [97] D L Connolly, *Visualization of vertical hydrocarbon migration in seismic data: Case studies from the Dutch North Sea*, *Interpretation* **3**, 21 (2015).
- [98] J S Jordan, M A Hesse, J F Rudge, *On mass transport in porosity waves*, *Earth Planet. Sci. Lett.* **485**, 65 (2018).
- [99] G A Peshkov, L A Khakimova, E V Grishko, M Wangen, V M Yarushina, *Coupled basin and hydro-mechanical modeling of gas chimney formation: The SW Barents Sea*, *Energies* **14**, 6345 (2021).
- [100] L Räss, V M Yarushina, N S C Simon, Y Y Podladchikov, *Chimneys, channels, pathway flow or water conducting features - An explanation from numerical modelling and implications for CO₂ storage*, *Energy Proc.* **63**, 3761 (2014).
- [101] L Räss, N S C Simon, Y Y Podladchikov, *Spontaneous formation of fluid escape pipes from subsurface reservoirs*, *Sci. Rep.* **8**, 11116 (2018).
- [102] G C Richard, S Kanjilal, H Schmeling, *Solitary-waves in geophysical two-phase viscous media: A semi-analytical solution*, *Phys. Earth Planet. Int.* **198**, 61 (2012).
- [103] M Tian, J J Ague, *The impact of porosity waves on crustal reaction progress and CO₂ mass transfer*, *Earth Planet. Sci. Lett.* **390**, 80 (2014).
- [104] V M Yarushina, Y Y Podladchikov, *(De)compaction of porous viscoelastoplastic media: Model formulation*, *J. Geophys. Res. Sol. Earth* **120**, 4146 (2015).
- [105] V M Yarushina, Y Y Podladchikov, J A D Connolly, *(De)compaction of porous viscoelastoplastic media: Solitary porosity waves*, *J. Geophys. Res. Sol. Earth* **120**, 4843 (2015).
- [106] D M Audet, A C Fowler, *A mathematical model for compaction in sedimentary basins*, *Geophys. J. Int.* **110**, 577 (1992).
- [107] V Barcion, F M Richter, *Nonlinear-waves in compacting media*, *J. Fluid Mech.* **164**, 429 (1986).
- [108] J A D Connolly, Y Y Podladchikov, *Temperature-dependent viscoelastic compaction and compartmentalization in sedimentary basins*, *Tectonophysics* **324**, 137 (2000).
- [109] J Dohmen, H Schmeling, J P Kruse, *The effect of effective rock viscosity on 2-D magmatic porosity waves*, *Solid Earth* **10**, 2103 (2019).
- [110] J A D Connolly, Y Y Podladchikov, *Decompaction weakening and channeling instability in ductile porous media: Implications for asthenospheric melt segregation*, *J. Geophys. Res. Sol. Earth* **112**, 10205 (2007).
- [111] L Räss, T Duretz, Y Y Podladchikov, *Resolving hydromechanical coupling in two and three dimensions: Spontaneous channelling of porous fluids owing to decompaction weakening*, *Geophys. J. Int.* **218**, 1591 (2019).

- [112] V M Yarushina, Y Y Podladchikov, H Wang, *Model for (de)compaction and porosity waves in porous rocks under shear stresses*, *J. Geophys. Res. Sol. Earth* **125**, e2020JB019683 (2020).
- [113] L I Dimitrov, *Mud volcanoes—the most important pathway for degassing deeply buried sediments*, *Earth Sci. Rev.* **59**, 49 (2002).
- [114] A J Kopf, *Making calderas from mud*, *Nat. Geosci.* **1**, 500 (2008).
- [115] S Zhong, J Zhang, J Luo, Y Yuan, P Su, *Geological characteristics of mud volcanoes and diapirs in the Northern Continental Margin of the South China Sea: Implications for the mechanisms controlling the genesis of fluid leakage structures*, *Geofluids* **2021**, 5519264 (2021).
- [116] F Dubois, M Jean, M Renouf, R Mozul, A Martin, *et al.*, *LMGC90. 10e colloque national en calcul des structures*, hal-00596875, Giens (France) (2011).
- [117] F Dubois, R Mozul, *LMGC90. 11e colloque national en calcul des structures*, hal-01717115, Giens (France) (2013).
- [118] M Constant, N Coppin, F Dubois, V Vidal, V Legat, J Lambrechts, *Simulation of air invasion in immersed granular beds with an unresolved FEM-DEM model*, *Comput. Par. Mech.* **8**, 535 (2020).
- [119] R Mourgues, P R Cobbold, *Some tectonic consequences of fluid overpressures and seepage forces as demonstrated by sandbox modelling*, *Tectonophysics* **376**, 75 (2003).
- [120] P Horsrud, E F Sonstebo, R Boe, *Mechanical and petrophysical properties of North Sea shales*, *Int. J. Rock Mech. Min.* **35**, 1009 (1998).
- [121] M Wangen, *A 3D model for chimney formation in sedimentary basins*, *Comp. Geosci.* **137**, 104429 (2020).
- [122] M Huuse, S J Shoulders, D I Netoff, J Cartwright, *Giant sandstone pipes record basin-scale liquefaction of buried dune sands in the Middle Jurassic of SE Utah*, *Terra Nova* **17**, 80 (2005).
- [123] K S Roberts, R J Davies, S A Stewart, *Structure of exhumed mud volcano feeder complexes, Azerbaijan*, *Basin Res.* **22**, 439 (2010).
- [124] J M Valverde, A Castellanos, *Types of gas fluidization of cohesive granular materials*, *Phys. Rev. E* **75**, 031306 (2007).
- [125] M Warsitzka, N Kukowski, F May, *Fluid-overpressure driven sediment mobilisation and its risk for the integrity for CO₂ storage sites - An analogue modelling approach*, *Energy Procedia* **114**, 3291 (2017).
- [126] O Galland, G R Gisler, Ø T Haug, *Morphology and dynamics of explosive vents through cohesive rock formations*, *J. Geophys. Res. Sol. Earth* **119**, 4708 (2014).
- [127] A Seiphoori, A Gunn, S Kosgodagan Acharige, P E Arratia, D J Jerolmack, *Tuning sedimentation through surface charge and particle shape*, *Geophys. Res. Lett.* **48**, e2020GL091251 (2021).